Biochemical and Biophysical Research Communications 451 (2014) 541–547

Contents lists available at ScienceDirect

Biochemical and Biophysical Research Communications

journal homepage: www.elsevier.com/locate/ybbrc

Introducing transglycosylation activity in *Bacillus licheniformis* α-amylase by replacement of His235 with Glu

Phuong Lan Tran [a,1], Hyun-Ju Cha [b,1], Jin-Sil Lee [a], Sung-Hoon Park [c], Eui-Jeon Woo [d], Kwan-Hwa Park [a,e,*]

[a] Department of Foodservice Management and Nutrition, Sangmyung University, 7 Hongji-dong, Jongno-gu, Seoul 110-743, Republic of Korea
[b] Division of Industrial Promotion Research, Korea Food Research Institute, 62 Anyangpangyo-ro 1201 beon-gil, Bundang-gu, Seongnam-si, Gyeonggi-do 463-746, Republic of Korea
[c] Lee Gil Ya Cancer and Diabetes Institute, Gachon University of Medicine and Scienece, 7-45 Songdo-dong, Yeonsu-ku, Incheon 406-840, Republic of Korea
[d] Medical Proteomics Research Center, Korea Research Institute of Bioscience and Biotechnology (KRIBB), 125 Gwahak-ro, Yuseong-gu, Daejeon 305-806, Republic of Korea
[e] Department of Food Science and Biotechnology, Seoul National University, Seoul 151-742, Republic of Korea

ARTICLE INFO

Article history:
Received 25 July 2014
Available online 10 August 2014

Keywords:
Bacillus licheniformis thermostable α-amylase
Substrate transglycosylation
Site-directed mutagenesis
Transfer product
Binding-subsite mapping

ABSTRACT

To understand the role of His and Glu in the catalytic activity of *Bacillus licheniformis* α-amylase (BLA), His235 was replaced with Glu. The mutant enzyme, H235E, was characterized in terms of its mode of action using labeled and unlabeled maltooctaose (Glc8). H235E predominantly produced maltotridecaose (Glc13) from Glc8, exhibiting high substrate transglycosylation activity, with K_m = 0.38 mM and k_{cat}/K_m = 20.58 $mM^{-1}\,s^{-1}$ for hydrolysis, and K_{m2} = 18.38 mM and k_{cat2}/K_{m2} = 2.57 $mM^{-1}\,s^{-1}$ for transglycosylation, while the wild-type BLA exhibited high hydrolysis activity exclusively. Glu235—located on a wide open groove near subsite +1—is likely involved in transglycosylation via formation of an α-1,4-glycosidic linkage and may recognize and stabilize the non-reducing end glucose of the acceptor molecule.

1. Introduction

Most members of α-amylases (EC 3.2.1.1) belonging to family 13 (GH13) catalyze hydrolysis of α-1,4-glycosidic linkages in starch [1]. In addition to hydrolysis activity, the enzyme exhibits transglycosylation activities, albeit to a lesser degree, at high substrate concentrations [2,3]. Moreover, α-amylases show multiple modes of action in which the enzyme cleaves the α-1,4 linkage of glucan randomly and in multiple ways. These complex modes of action make difficult prediction of the reaction rates and products of α-amylases in starch conversion. The catalytic activity and substrate specificity of such enzymes have been investigated to increase their stability at high temperatures and to alter the operative pH ranges suitable for industrial purposes using protein engineering [4–6]. Therefore, development of a model of the hydrolysis and transglycosylation activities of α-amylase on a molecular and kinetic basis is desirable. In our previous study of thermostable *Bacillus licheniformis* α-amylase [7], we performed nine-subsite mapping by means of kinetic analysis: six in the terminal nonreducing-end-binding site and three at the reducing-end-binding region of BLA. Unlike other typical amylases, such as BLA, which transfer a glucan moiety to C4-OH, forming an α-1,4 linkage, maltogenic amylases (MAases: GH13) exhibit transglycosylation of a glucan moiety to the C6-hydroxyl groups of acceptor molecules to form an α-1,6-glycosidic linkage [8]. The 3-D structure of the maltogenic amylase showed that an extra space, absent from other typical α-amylases, is present at the bottom of the active site cleft; moreover, the Glu332 residue in this space was identified to be important for transglycosylation [8]. Additionally, we reported that the amino acid in the second region was conserved as glutamic acid (corresponding to E332 in the *Thermus* maltogenic amylase, ThMA), compared to histidine in α-amylases (Table 1) [9–17]. The replacement of glutamate with histidine in MAases reduced the transglycosylation activity [8,14]. It has been suggested that glutamate plays a role in transglycosylation. Cha et al. showed that an increase in the hydrophobicity between the third and fourth conserved regions enhanced the transglycosylation activity of MAases [14]. However, Kim et al. investigated the transglycosylation of dimeric MAases the oligomeric states of which differ from those of typical monomeric α-amylases [8]. The space "extra sugar-binding space" formed between two subunits of MAases could provide room for an accep-

* Corresponding author. Fax: +82 2 391 8758.
E-mail address: parkkwanhwa@gmail.com (K.-H. Park).
[1] These authors equally contributed to this study.

http://dx.doi.org/10.1016/j.bbrc.2014.08.019
0006-291X/

Table 1
Alignment of amino acid residues in conserved regions of GH13 amylases.

Enzyme	Major function	Conserved regions					Ref.
		I		II	III	IV	
				* o			
Bacillus licheniformis	Hydrolysis of	------	228	GFRLDAVKH	----	------	[9]
Bacillus stearothermophilus	α-1,4-glycosidic	------	230	GFRLDGLKH	----	------	[10]
Aspergillus oryzae	linkage	------	202	GIRIDTVKH	----	------	[11]
Barley		------	127	DGRLDWGPH	----	------	[12]
Thermus strain IM6501	Hydrolysis and Transglycosylation of α-1,4- or -1,6 glycosidic linkage	------	324	GWRLDVANE	----	------	[13]
Bacillus stearothermophilus		------	324	GWRLDVANE	----	------	[14]
Bacillus subtilis		------	323	GWRLDVANE	----	------	[15]
Thermoactinomyces vulgaris		------	321	GWRLDVANE	----	------	[16]
Bacillus sp. I-5		------	321	GWRLDVANE	----	------	[17]

*Catalytic site; °substrate binding site.

tor molecule at the location of Glu332 in the second conserved region (corresponding to His235 in BLA). Furthermore, the amino acid residues in an analogous position (corresponding to His235 in BLA) in *Thermotoga maritima* were replaced by various amino acid residues, which enhanced the alcoholytic or transglycosylation activity [18]. Therefore, investigation of the role of the histidine or glutamate in that position may provide insight into the mechanism of transglycosylation and hydrolysis in the GH 13 family. However, Tran et al. recently proposed a 9-substrate binding subsite of BLA [7]. Thus, the mechanism underlying the transglycosylation and hydrolysis activities of BLA could be better understood on the basis of subsite mapping and product analyses.

Therefore, we investigated the mode of action and kinetics of the transglycosylation and hydrolysis activities of the mutant enzyme, His235Glu. Finally, we discussed the transglycosylation reaction involving the formation of the α-1,4-glycosidic linkage on a molecular structural basis.

2. Materials and methods

2.1. Construction of mutant BLA

Site-directed mutagenesis was performed using a QuikChange™ site-directed mutagenesis kit (Stratagene, USA). The recombinant plasmid p6xHisBLA, carrying the *bla* gene with six histidines at the N-terminus, was used as template DNA. The sequence of the synthetic oligonucleotide used for the introduction of H235E was 5′-CGGTTTCCGTCTAGATGCTGTCAAAGAGATTAA ATTTTCT-3′. The mutation introduced to BLA was confirmed using the dideoxy chain-termination sequencing method with an ABI377 PRISM DNA sequencer (Perkin-Elmer, USA).

2.2. Purification of BLA wild-type and mutant enzymes

Escherichia coli strain MC1061 was used as a host for wild-type and mutant BLA expression. Recombinant *E. coli* harboring the wild-type and mutant *bla* genes with six histidines at the N-terminus were cultured overnight at 37 °C by shaking in Luria–Bertani (LB) medium containing ampicillin (100 μg/ml) or kanamycin (25 μg/ml) for wild-type or mutant BLA, respectively. The wild-type and mutant BLAs were purified using nickel (Ni^{2+}) nitrilotriacetic acid (Ni–NTA) resin (Qiagen, Hilden, Germany) packed in a Poly-Prep® chromatography column (Bio-Rad, Hercules, CA, USA) as described by Park et al. [19]. The purity of the enzymes was confirmed by SDS–PAGE analysis.

2.3. Enzyme activity determination

Wild-type and mutant BLA activities were assayed according to the dinitrosalicylic acid (DNS) method [20] by quantifying reducing sugar production by the enzyme. One unit of BLA activity was defined as the amount of enzyme that produced 1 mM equivalent of glycosidic bonds in the substrate in 1 min under the reaction conditions used.

2.4. Preparation of ^{14}C-lebeled maltooctaose

Glc8 was kindly provided by Dr. Byung Cheol Min (Daesang Corporation, Korea). Glc8 labeled with 10 mCi/mmol ^{14}C-D-glucose at its reducing end was synthesized using ^{14}C-D-glucose and β-cyclodextrin and the Toruzyme coupling reaction (Novozyme, Bagsvaerd, Denmark) at 80 °C for 30 min [21]. The reaction product was separated by paper chromatography using acetonitrile/n-propanol alcohol/ethyl acetate/water (8.5:5:2:7, v/v/v/v) as the solvent.

2.5. Thin layer chromatography (TLC) analysis

TLC was conducted using a Whatman K5F silica gel plate with n-butanol/ethanol/water (5:3:3, v/v/v) as the solvent to confirm the reaction mode of the wild-type and mutant BLA enzymes in the presence of a high concentration of maltooctaose.

The TLC plate containing the reaction products of the mixture substrates Glc8 and ^{14}C-labeled Glc8 (4:1) with the mutant BLA was developed twice and then covered with an imaging plate in a cassette for 10 h. The reducing end radioactivity products were detected by scanning using a BAS2500 image analyzer (Fuji Film, Tokyo, Japan).

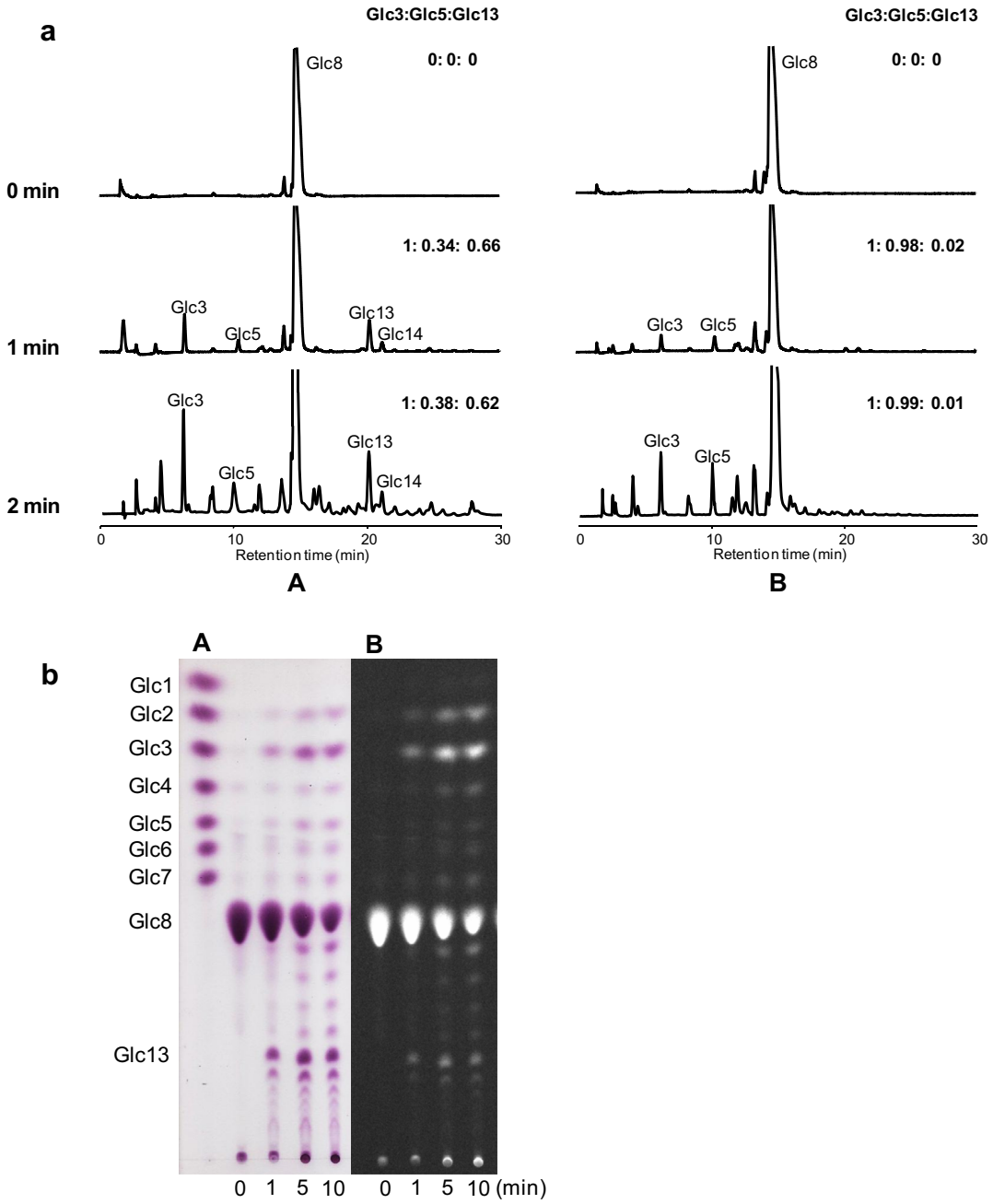

Fig. 1. (a) HPAEC analysis of the reaction products of mutant (A) and wild-type (B) BLA with Glc8. (b) TLC analysis of the reaction products of the mutant BLA with ^{14}C-labeled Glc8. The chromatogram was visualized using naphthol–H_2SO_4 (A) and autoradiography (B).

2.6. Analysis of reaction products by high-performance anion-exchange chromatography (HPAEC)

Wild-type and mutant BLA reactions were performed at 70 °C using 3.80–22.80 mM Glc8, stopped by 0.1 N NaOH and then analyzed using a HPAEC system (Dionex-300, Dionex, Sunnyvale, CA, USA) with an electrochemical detector (ED40, Dionex). The system was equipped with a CarboPac™ PA-1 anion-exchange column (250 × 4 mm, Dionex) connected to a guard column and run with a 0–0.6 M sodium acetate gradient in 0.15 M sodium hydroxide at a flow rate of 1.0 mL/min [20]. Product concentrations were determined using Glc3 and Glc5 standard curves. The maltooligosaccharides were identified and quantified by comparison of retention time and area with those of the corresponding standards (Glc1−Glc14).

2.7. Determination of transglycosylation and hydrolysis reaction rate constants

The reaction rate constants for hydrolysis and transglycosylation were determined using Glc8 as substrate based on two stages: The K_m and k_{cat} of hydrolysis were assessed at substrate concentrations of 0.20–1.20 mM, and the K_{m2} and the k_{cat2} of transglycosylation were determined at 3.80–22.80 mM. Substrate transglycosylation and hydrolysis kinetics were calculated using the minimal kinetic scheme for substrate transglycosylation as described previously

[22]. Substrate transglycosylation by H235E was considered to proceed as shown in Eq. (1) below:

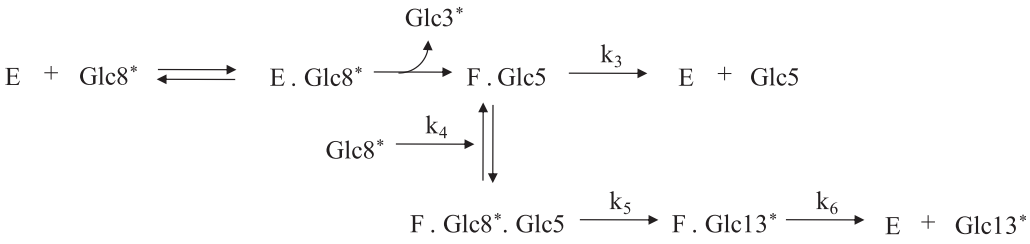

(scheme1)

where

k_3 is the rate constant of hydrolysis for which the formation of Glc5 is taken as the hydrolysis reaction.

k_4 is the transglycosylation reaction rate constant, which can be obtained by,

d(Glc13)/dt = d(Glc3–Glc5)/dt; hence the Glc13 standard curve is not available.

Thus

$$\bar{V}_{Glc3} = \frac{2k_{cat}K_{m2}[S] + k_{cat2}[S]^2}{K_m K_{m2} + K_{m2}[S] + [S]^2} \quad (1)$$

2.8. Molecular modeling

The Glc8 ligand complex model was initially constructed by the manual fitting of the Glc8 ligand into the active site of BLA based on the superposition of various lengths of carbohydrate ligands to α-amylases. Initial complex models were subjected to energy minimization followed by 1 ps of molecular dynamics at 3008 K after equilibration. They were minimized to a maximum derivative of 1.0 kcal per step using the Discover module in the Insight II software (Accelrys, San Diego, CA) with Amber force fields.

3. Results and discussion

3.1. Transglycosylation and hydrolysis modes of wild-type and mutant BLA

Non-labeled and ^{14}C-labeled maltooctaose (Glc8) at 22.80 mM were employed to investigate the transglycosylation and hydrolysis modes of wild-type and mutant BLA. The reaction products were subjected to HPAEC analysis using an image analyzer. Fig. 1a and b show that the wild-type enzyme produced Glc5 and Glc3 from Glc8 by hydrolysis, whereas H235E yielded Glc13 in addition to Glc5 and Glc3 by transglycosylation. The mutant BLA had high transglycosylation activity and produced a range of hydrolysis and transfer products, while the wild-type BLA exclusively produced hydrolysis products with only trace amounts of transfer products. Upon treatment of the reaction mixture with β-amylase, the major and minor peaks greater than Glc3 disappeared, indicating that the transfer products did not contain an α-1,6-glycosidic linkage (data not shown). It is likely that the mutant enzyme transferred a Glc5 moiety from Glc8 to another Glc8 acceptor by forming an α-1,4-glycosidic bond to form Glc13 (scheme 1). Furthermore, we can assume that Glc5 is the product solely of hydrolysis, Glc13 is the transglycosylated product, and Glc3 is a product of both hydrolysis and transglycosylation (scheme 1). As seen in Fig. 1a, in the reaction catalyzed by the mutant enzyme the ratio of the concentration of Glc3 to that of Glc5 approached 3:1, whereby Glc5 was partly transferred to form Glc13 and Glc3 was released. In contrast, that of the wild-type enzyme was approximately 1:1, indicating that Glc5 was not consumed for transglycosylation. Furthermore, as shown in Fig. 1b, labeled Glc3 and Glc13 were produced by both transglycosylation and hydrolysis, but radioactive Glc5 was hardly detected. Thus, H235E transferred the maltopentaosyl moiety (unlabeled) from the non-reducing end of Glc8 to another Glc8 acceptor containing labeled reducing end glucose, producing Glc13 and radioactivity (scheme 1). Also, the results above are in good agreement with the alcoholic (transglycosylation) activity of the mutant enzyme, which was enhanced by the replacement of His with Glu in the liquefying enzyme of *Bacillus stearothermophilus* and AmyA of *T. maritima* [18,23]. Therefore, glutamate at position 235 may play an important role in transglycosylation, as in the MAases, as reported previously [8].

3.2. The Glu235 residue near subsite +1 recognizes the non-reducing end glucose of acceptor glucan

We examined substrate transglycosylation with various maltooligosaccharides (Glc7–Glc9); the resultant products are shown

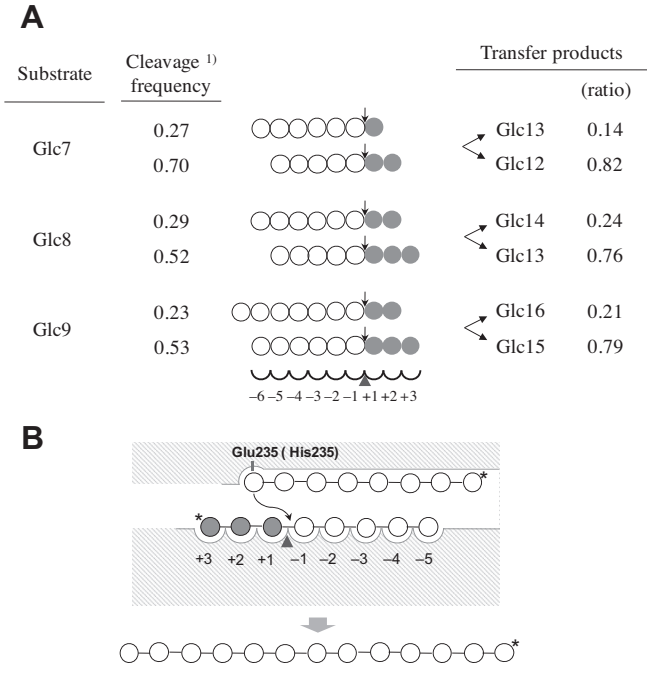

Fig. 2. (A) Schematic diagram of the transglycosylation mode of the BLA mutant H235E. (B) Comparison of the major transfer products in relation to cleavage frequency. 1)Cleavage frequency of wild-type BLA [7].

Table 2
Kinetic parameters of the BLA wild-type and H235E mutant for hydrolysis and transglycosylation with Glc8.

	Hydrolysis			Transglycosylation		
	K_m (mM)	k_{cat} (s^{-1})	k_{cat}/K_m ($mM^{-1}\ s^{-1}$)	K_{m2} (mM)	k_{cat2} (s^{-1})	k_{cat2}/K_{m2} ($mM^{-1}\ s^{-1}$)
Wild-type	0.39 ± 0.02	11.23 ± 0.16	28.80	ND	ND	ND
H235E	0.38 ± 0.04	7.82 ± 0.39	20.58	18.38 ± 0.92	47.30 ± 2.37	2.57

ND, not detected.

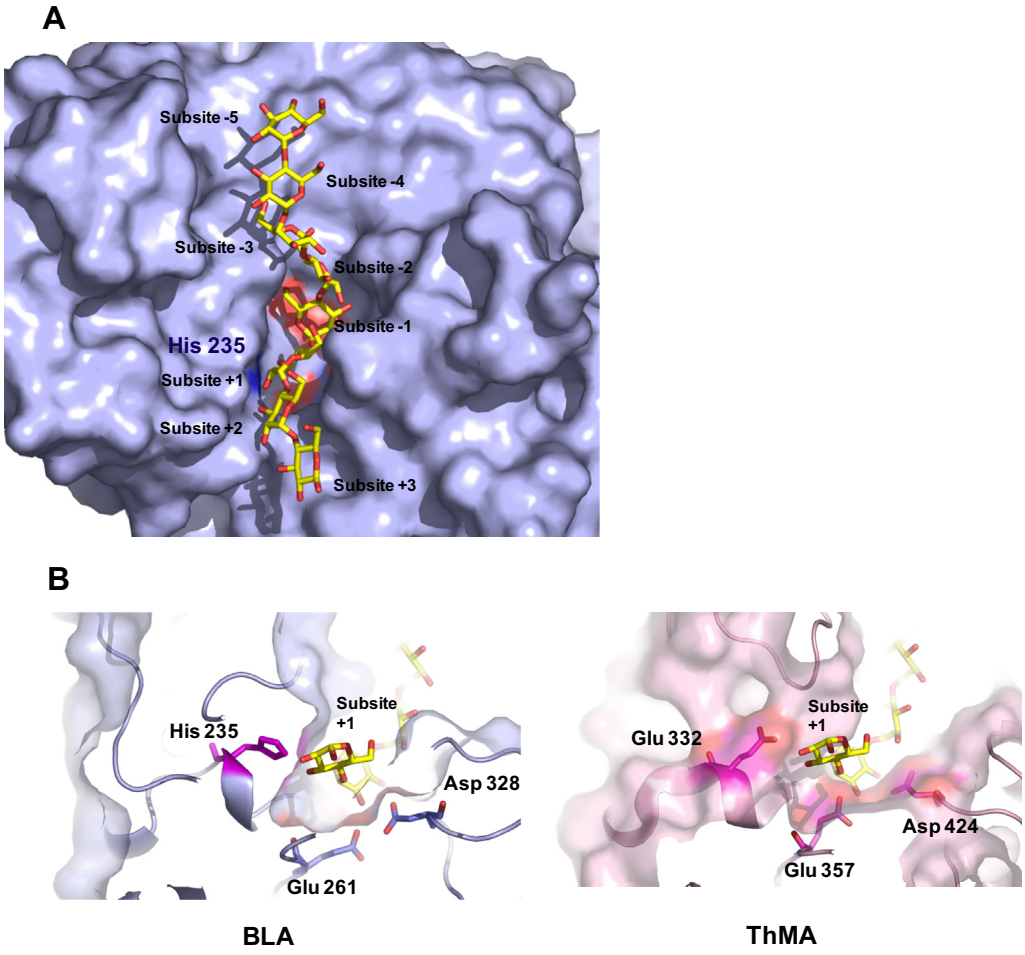

Fig. 3. (A) Surface representation of BLA with a hypothetical model of Glc8 substrate bound to the active site. His235 is colored blue. Residues in the active site are colored red. (B) Surface diagrams of subsite +1 in BLA and ThMA. The catalytic residues Glu261 and Asp328 in BLA and Glu357, and Asp424 in ThMA, are shown as sticks. Protruding geometry at subsite +1 in ThMA with Glu332 is highlighted. A hypothetical model of the Glc8 substrate in BLA; the same substrate is drawn in ThMA for comparison.

schematically in Fig. 2A. The products of Glc8 hydrolysis by the wild type were identified as two pairs: Glc3 & Glc5 and Glc2 & Glc6, which had cleavage affinities of 0.52 and 0.29, respectively [7]. In the case of the mutant enzyme, Glc5 or Glc6 positioned at binding sites −5 and −1 or −6 and −1 of H235E were transferred to the non-reducing end glucose of another Glc8 molecule, yielding Glc13 and Glc14 as transfer products at ratios of 0.76 and 0.24, respectively. Similarly, Glc9 was converted into Glc3 and Glc6 as the major pair products of hydrolysis, whereby the Glc6 placed at binding sites −6 and −1 was transferred to another Glc9 acceptor, producing Glc15 at a ratio of 0.79 (Fig. 2A). Consistent with cleavage frequency-dependent transfer modes, the mutant exhibited significantly enhanced transglycosylation in terms of the formation of an α-1,4-glycosidic linkage. In contrast, ThMA transfers the maltosyl moiety C6-OH of the non-reducing end glucose molecule via formation of an α-1,6-glycosidic linkage [8]. Unlike ThMA, the H235E mutant transfers a glucan moiety to C4-OH of the non-reducing end of an acceptor, forming an α-1,4-glycosidic linkage.

3.3. Kinetic parameters of the mutant H235E

To evaluate its kinetics, the wild-type or mutant enzyme was added to a Glc8 solution of various concentrations (0.20–1.20 mM for hydrolysis and 3.80–22.80 mM for substrate transglycosylation), and the reaction products were quantified by HPAEC under the assumption that Glc5 is solely the product of hydrolysis and Glc3 is the product of both hydrolysis and transglycosylation (scheme 1). As shown in Table 2, the K_m for the hydrolysis reaction

of the mutant enzyme was 0.38 mM, which is not significantly different from the 0.39 mM of the wild-type, but k_{cat} was reduced from 11.23 s^{-1} to 7.82 s^{-1}. Consequently, the specificity constant k_{cat}/K_m of the mutant enzyme was lower than that of the wild-type enzyme. However, the mutant enzyme exhibited high transfer activity at substrate concentrations greater than 3.80 mM. The kinetic parameters for transglycosylation of H235E were K_{m2} = 18.38 mM, k_{cat2} = 47.30 s^{-1} and k_{cat2}/K_{m2} = 2.57 mM^{-1} s^{-1}. On the contrary, the wild-type enzyme showed a trace amount of the transfer product even at high concentrations of substrate. As the amount of Glc5 produced solely by the hydrolysis reaction of the wild-type enzyme was almost identical to the amount of Glc3 released by both hydrolysis and transglycosylation (Fig. 1a), we failed to obtain data for transglycosylation (Table 2), indicating that the wild-type BLA catalyzed exclusively the hydrolysis reaction.

3.4. Molecular modeling of H235E: structural geometry is implicated in the formation of an α-1,4-glycosidic linkage by transglycosylation

The Glc8 substrate is shown superimposed on the structure of BLA in Fig. 3A and surface diagrams for subsite +1 in H235E and ThMA are compared in Fig. 3B. Substitution of His235 for Glu235 in BLA resulted in a marked increase in transfer activity (Table 2 and Fig. 1a). Therefore, Glu235 appears to play an important role in the binding of another Glc8 molecule as an acceptor. Molecular modeling using the substrate Glc8 revealed a groove surface that is wide open beyond the subsite. The transglycosylation reaction could occur in a similar manner as observed in MAases [8]. Firstly, Glc8 occupies the +3 to −5 subsites at the active site of H235E, and then the second Glc8 as acceptor molecule enters the +1 subsite where the wide open geometry provides space at the −1 to −5 subsites to accommodate the acceptor Glc8. The enzyme catalyzes the transfer of Glc5 occupying the glycone subsite (−1 to −5) to the non-reducing end glucose with formation of an α-1,4-linked transfer product. The location of the His235 or Glu235 residue close to subsite +1 and its highly conserved sequence in homologs that show transfer activity suggest that Glu235 has a functional role in the stabilizing and binding of acceptor molecules for transfer activity. In general, α-1,6-glycosidases have a narrow and twisted geometry around the active-site entrance at subsite +1, which can accommodate an α-1,6-glycosidic bond, while that of α-1,4-glycosidase is wide open and straight [24–27], as shown in Fig 3B. Comparison of active sites near subsite +1 shows that the protruding geometry and the narrow groove at subsite +1 in ThMA are involved in the stabilization of the substrate molecule and necessary for α-1,6-transfer activity [28]. In contrast, the subsite +1 of H235E is located in a wide-open geometry, resulting in an α-1,4-transfer mode. Similarly, AmyB shows a wide cavity that recognizes the non-reducing end of the substrate [24,29]. Thus, in H235E the Glu235 in a wide open geometry near subsite +1 may play a role in recognition of the non-reducing end glucose and stabilization of the transfer reaction by electrostatic interactions with the non-reducing end of acceptor molecules, resulting in the formation of an α-1,4-glycosidic linkage.

Acknowledgments

This study was supported in part by the Basic Research Program through the National Research Foundation (2012R1A1A2005012) and in part by the Next Generation BioGreen21 Program (SSAC, No. PJ009086), Rural Development Administration, Republic of Korea.

References

[1] B. Henrissat, I. Callebaut, S. Fabrega, P. Lehn, J.P. Mornon, G. Davies, Conserved catalytic machinery and the prediction of a common fold for several families of glycosyl hydrolases, Proc. Natl. Acad. Sci. USA 92 (1995) 7090–7094.
[2] A.E. Habibi, K. Khajeh, M. Nemat-Gorgani, Chemical modification of lysine residues in *Bacillus licheniformis* α-amylase: conversion of an *endo*- to an *exo*-type enzyme, J. Biochem. Mol. Biol. 37 (2004) 642–647.
[3] M.H. Rivera, A. López-Munguía, X. Sobern, G. Saab-Rincón, α-Amylase from *Bacillus licheniformis* mutants near to the catalytic site: effects on hydrolytic and transglycosylation activity, Protein Eng. 16 (2003) 504–514.
[4] N. Declerck, M. Machius, R. Chambert, G. Wiegand, R. Huber, C. Gaillardin, Hyperthermostable mutants of *Bacillus licheniformis* α-amylase: thermodynamic studies and structural interpretation, Protein Eng. 10 (1997) 541–549.
[5] N. Declerk, M. Machius, P. Joyet, G. Wiegand, R. Huber, C. Gaillardin, Hyperthermostabilization of *Bacillus licheniformis* α-amylase and modulation of its stability over a 50 °C temperature range, Protein Eng. 16 (2003) 287–293.
[6] A. Shaw, R. Bott, A.G. Day, Protein engineering of α-amylase for low pH performance, Curr. Opin. Biotechnol. 10 (1999) 349–352.
[7] P.L. Tran, J.S. Lee, K.H. Park, Experimental evidence for a 9-binding subsite of *Bacillus licheniformis* thermostable α-amylase, FEBS Lett. 588 (2014) 620–624.
[8] T.J. Kim, C.S. Park, H.Y. Cho, S.S. Cha, J.S. Kim, S.B. Lee, T.W. Moon, J.W. Kim, B.H. Oh, K.H. Park, Role of the glutamate 332 residue in the transglycosylation activity of *Thermus* maltogenic amylase, Biochemistry 39 (2000) 6773–6780.
[9] N. Declerck, M. Machius, P. Joyet, G. Wiegand, R. Huber, C. Gaillardin, Engineering the thermostability of *Bacillus licheniformis* α-amylase, Biol. Brat. 11 (2002) 203–211.
[10] H. Ihara, T. Sasaki, A. Tsuboi, H. Yamagata, N. Tsukagoshi, S. Udaka, Complete nucleotide sequence of a thermophilic α-amylase gene: homology between prokaryotic and eukaryotic α-amylases at the active sites, J. Biochem. 98 (1985) 95–103.
[11] H. Toda, K. Kondo, K. Narita, The complete amino acid sequence of taka-amylase A, Proc. Jpn. Acad. 58 (1982) 208–212.
[12] J.C. Rogers, C. Milliman, Isolation and sequence analysis of a barley α-amylase cDNA clone, J. Biol. Chem. 258 (1983) 8169–8174.
[13] T.J. Kim, M.J. Kim, B.C. Kim, J.C. Kim, T.K. Cheong, J.W. Kim, K.H. Park, Modes of action of acarbose hydrolysis and transglycosylation catalyzed by a thermostable maltogenic amylase, the gene for which was cloned from a *Thermus* strain, Appl. Environ. Microbiol. 65 (1999) 1644–1651.
[14] H.J. Cha, H.G. Yoon, Y.W. Kim, H.S. Lee, J.W. Kim, K.S. Kweon, B.H. Oh, K.H. Park, Molecular and enzymatic characterization of a maltogenic amylase that hydrolyzes and transglycosylates acarbose, Eur. J. Biochem. 253 (1998) 251–262.
[15] F. Li, X. Zhu, Y. Li, H. Cao, Y. Zhang, Functional characterization of a special thermophilic multifunctional amylase OPMA-N and its N-terminal domain, Acta Biochim. Biophys. Sin. (Shanghai) 43 (2011) 324–334.
[16] T. Tonozuka, M. Ohtsuka, S. Mogi, H. Sakai, T. Ohta, Y. Sakano, A neopullulanase-type α-amylase gene from *Thermoactinomyces vulgaris* R-47, Biosci. Biotechnol. Biochem. 57 (1993) 395–401.
[17] T.J. Kim, J.H. Shin, J.H. Oh, M.J. Kim, S.B. Lee, S. Ryu, K. Kwon, J.W. Kim, E.H. Choi, J.F. Robyt, K.H. Park, Analysis of the gene encoding cyclomaltodextrinase from alkalophilic *Bacillus* sp. I-5 and characterization of enzymatic properties, Arch. Biochem. Biophys. 353 (1998) 221–227.
[18] J.Y. Damián-Almazo, A. Moreno, A. López-Munguía, X. Soberón, F. González-Muñoz, G. Saab-Rincón, Enhancement of the alcoholytic activity of α-amylase AmyA from *Thermotoga maritima* MSB8 (DSM 3109) by site-directed mutagenesis, Appl. Environ. Microbiol. 74 (2008) 5168–5177.
[19] J.H. Park, H.J. Kim, Y.H. Kim, H. Cha, Y.W. Kim, T.J. Kim, Y.R. Kim, K.H. Park, The action mode of *Thermusaquaticus* YT-1 4-α-glucanotransferase and its chimeric enzymes introduced with starch-binding domain on amylose and amylopectin, Carbohydr. Polym. 67 (2007) 164–173.
[20] G.L. Miller, Use of dinitrosalycylic acid reagent for determination by reducing sugar, Anal. Chem. 31 (1959) 426–428.
[21] J.F. Robyt, D. French, The action pattern of porcine pancreatic α-amylase in relationship to the substrate binding site of the enzyme, J. Biol. Chem. 245 (1970) 3917–3927.
[22] D.H.D. Nguyen, J.T. Park, J.H. Shim, P.L. Tran, E.F. Oktavina, T.L.H. Nguyen, S.J. Lee, C.S. Park, D. Li, S.H. Park, D. Stapleton, J.S. Lee, K.H. Park, Reaction kinetics of substrate transglycosylation catalyzed by Trex of *Sulfolobus solfataricus* and effects on glycogen breakdown, J. Bacteriol. 196 (2014) 1941–1949.
[23] G. Saab-Rincón, G. del-Río, R.I. Santamaría, A. López-Munguía, X. Soberón, Introducing transglycosylation activity in a liquefying α-amylase, FEBS Lett. 453 (1999) 100–106.
[24] K.H. Park, J.H. Jung, S.G. Park, M.E. Lee, J.F. Holden, C.S. Park, E.J. Woo, Structure features underlying the selective cleavage of a novel exo-type maltose-forming amylase from *Pyrococcus* sp, ST04, Acta Crystallogr. D70 (2014) 1659–1668.
[25] K. Yamamoto, H. Miyake, M. Kusunoki, S. Osaki, Crystal structures of isomaltase from *Saccharomyces cerevisiae* and in complex with its competitive inhibitor maltose, FEBS J. 277 (2010) 4205–4214.

[26] A. Abe, H. Yoshida, T. Tonozuka, Y. Sakano, S. Kamitori, Complexes of *Thermoactinomyces vulgaris* R-47 α-amylase 1 and pullulan model oligossacharides provide new insight into the mechanism for recognizing substrates with α-(1,6) glycosidic linkages, FEBS J. 272 (2005) 6145–6153.
[27] T. Pijning, A. Vujicic-Zagar, S. Kralj, L. Dijkhuizen, B.W. Dijkstra, Structure of the α-1,6/α-1,4-specific glucansucrase GTFA from *Lactobacillus reuteri* 121, Acta Crystallogr. F68 (2012) 1448–1454.
[28] J.T. Park, H.N. Song, T.Y. Jung, M.H. Lee, S.G. Park, E.J. Woo, K.H. Park, A novel domain arrangement in a monomeric cyclodextrin-hydolyzing enzyme from the hyperthermophiles *Pyrococcus furiosus*, Biochim. Biophys. Acta 2013 (1834) 380–386.
[29] S.Y. Jun, J.S. Kim, K.H. Choi, J. Cha, N.C. Ha, Structure of a novel α-amylase AmyB from *Thermotoga neapolitana* that produces maltose from the nonreducing end of polysaccharides, Acta Crystallogr. D69 (2013) 442–450.